

Photocatalytic oxidation activity of titanium dioxide film enhanced by Mn non-uniform doping

ZHANG Kai-jian(张开坚)^{1,3}, XU Wei(徐 伟)^{2,4}, LI Xin-jun(李新军)²,
ZHENG Shao-jian(郑少健)², XU Gang(徐 刚)², WANG Jian-hua(王建华)⁴

1. College of Economy, Industry and Business Management, Chongqing University, Chongqing 400044, China;
2. Guangzhou Institute of Energy Conversion, Chinese Academy of Sciences, Guangzhou 510640, China;
3. Panzhihua Iron & Steel Research Institute, Panzhihua Iron & Steel Ltd Co, Panzhihua 617000, China;
4. No.719 Research Institute of China Shipbuilding Industry Corporation, Wuhan 430064, China

Received 20 February 2006; accepted 26 March 2006

Abstract: The thin films of TiO₂ doped by Mn non-uniformly were prepared by sol-gel method under process control. Each film was characterized by XPS, SEM, UV-vis spectrophotometry and electrochemistry workstation analysis. The activity of the photocatalyst was evaluated by the kinetics of photocatalytic degradation of aqueous methyl orange under the UV radiation. The results show that Mn non-uniform doping evidently enhances the photocatalytic activity of TiO₂ thin film. In 80 min, the degradation rates of aqueous methyl orange are 62%, 12% and 34% for Mn non-uniformly doped film (0.7%), the uniformly doped film (0.7%) and pure titanium dioxide film, respectively. The characteristic of PN junction in the film was proved by electrochemical characterization. A mechanism for enhanced photocatalytic activity of Mn non-uniformly doped titanium dioxide film was discussed based on the effective separation of the photon-generated carrier because of the existence of the PN junction.

Key words: photocatalyst; TiO₂; Mn; non-uniform doping; film

1 Introduction

Heterogeneous photocatalysis is an effective technique for reducing the concentration of pollutants at low concentration. It has been demonstrated that almost all organics can be oxidized to generate carbon dioxide, water and simple mineral acids at room temperature on TiO₂ catalysts. TiO₂ photocatalysis has been extensively studied for its application in the environmental remediation processes[1–3]. However, the application of this material is compromised by its low photocatalytic efficiency. In order to enhance the activity of TiO₂, many scientists have attempted to modify TiO₂. The efforts have included noble metal loading, semiconductor composite and metal ion doping[4–6]. The method of metal ion doping is widely used, and almost all transitional metal ions have been reported[7,8]. However, few studies on titanium dioxide doped by Mn have been reported. Some reports demonstrated that the presence of many metal ions in the TiO₂ photocatalyst had a detrimental effect on its photocatalytic activity[9,10].

The heterogeneous photocatalytic oxidation efficiency depends on the quantity of the holes on the film surface, which react with the organic substance or the surface H₂O[11]. To increase the activity, more photon-generated carriers should be excited easily in the photocatalyst; then the carriers can separate effectively, and the carriers can migrate onto the surface before recombination of the carriers. Based on the theory that the space-charged region of the PN junction can hold back the recombination of the electron-hole pairs, we designed the thin films of TiO₂ doped by Mn with non-uniform distribution and prepared by sol-gel method under process control. The existence of a PN junction inside the Mn non-uniformly doped film was proved by its electrochemistry performance. As we expected, the photocatalytic activity of TiO₂ was enhanced evidently by Mn ion non-uniform doping (According to the preparation process, the preceding metal ion doping of TiO₂ should be defined as metal ion uniform doping, i.e. the distribution of metal ions in TiO₂ is uniform). A mechanism for enhanced photocatalytic activity of the Mn non-uniformly doped titanium dioxide film was

discussed.

2 Experimental

2.1 Preparation of Mn-doped and pure TiO₂ films

2.1.1 TiO₂-sol

The sol was prepared by the following method[12]. 68 mL of tetra-butyl-ortho-titanate and 16.5 mL of diethanolamine were dissolved in 210 mL absolute ethanol, and the mixture was then stirred vigorously for 1 h (Solution A). While stirring, the mixture of 3.6 mL of water and 100 mL of absolute ethanol (Solution B) was added drop-wise into Solution A. The resulting alkoxide solution was left in the dark for 24 h to form the TiO₂-sol.

2.1.2 Mn/TiO₂-sol

The preparation of Mn/TiO₂-sol was similar to the preparation of TiO₂-sol. The only difference was that various amounts of Mn(NO₃)₂ (analytical reagent) were added into 3.6 mL of H₂O to make various concentrations of sol when Solution B was made. Each different concentration of Mn/TiO₂ sol (mole fraction: 0.2%, 0.5%, 0.7%, 1.0%, 1.5%) was designated as MTx (x=0.2, 0.5, 0.7, 1.0, 1.5).

Samples of the doped or pure TiO₂ films formed on the soda lime glass substrates, which had been pre-coated with two SiO₂ layers, were prepared from the TiO₂ sol or Mn/TiO₂ sol by the following steps: 1) dipping-withdrawing at a speed of 2 mm/s; 2) drying at 100 °C for 10 min; 3) heating to 500 °C at the heating rate of 2 °C/s; 4) keeping at 500 °C for 1 h, then cooling. The films of TiO₂ in different doping modes described in Table 1 were prepared by repeating the above steps.

Table 1 Doping mode of TiO₂

Sample	Composing		
TT		4 layers TiO ₂ -sol	4 layers TiO ₂ -sol
MM	2 layers SiO ₂ -sol	4 layers Mn/TiO ₂ -sol	4 layers Mn/TiO ₂ -sol
MT		4 layers Mn/TiO ₂ -sol	4 layers TiO ₂ -sol

2.2 Characterization

The thickness of each TiO₂ film was measured by scanning electron microscopy (SEM; type S-520). The XPS spectra were acquired with an energy spectrometer (type PHI-5800) with a Mg K_α X-ray source operated at 15 keV and 18 mA. Each binding energy was referenced to the C1s at 284.6 eV. The crystal form of the film was obtained by X-ray diffraction(XRD) using a diffractometer (type D/MAX-III_A,) with Cu K_α radiation, with 30 kV of accelerating voltage and 30 mA of current, respectively. The resulted film was anatase, according to Ref.[6]. The spectral analyses of TiO₂ films were carried out with a UV-3010 UV-visible spectrophotometer, and

the baseline was based on a piece of SLG with one SiO₂ layer.

2.3 Electrochemistry experiments

Electrochemistry is an effective tool to study the material properties, such as chemistry (especially electrochemistry) processes and the mechanisms of interface reaction. The properties of photocatalytic films were analyzed using a CHI660 electrochemical station.

2.3.1 Preparation of film electrode

The photocatalysis film electrode (20 mm×20 mm) was prepared as described in section 2.1 (no SiO₂ layer), after the ITO conductive glass was washed in the base solution by ultrasonic vibrations.

2.3.2 Test of electrochemistry

Electrochemistry tests were performed in a three electrode system made of quartz cells linked to a CHI660 electrochemical station. TiO₂/ITO electrode served as the working electrode(WE); a platinum sheet (20 mm×20 mm) and a saturation calomel electrode(SCE) served as the counter electrode(CE) and the reference electrode, respectively. The electrolyte was 0.5 mol/L Na₂SO₄ aqueous solution prepared by analytical reagents and distilled water. The lamp-house of the photo electrochemical test was a tungsten lamp (5 W, λ_p=365 nm). All tests were carried out at room temperature.

2.4 Photocatalytic activity test

The reactor was a glass cylinder (d=70 mm, H=240 mm), in which five pieces of glass with photocatalysis film were settled tightly near the container inside the wall. Then, 400 mL of aqueous methyl-orange (10 mg/L in reverse osmosis-treated water, pH=5.9) was added into the cylinder, and the solution was aerated for 30 min before the experiment began. A high-pressure mercury lamp (125 W, λ_p=365 nm), was preheated for 30 min and placed in the reactor center as a light-house. The reactor was immersed in a thermostatic bath in order to obtain a constant temperature. The solution was sampled at an interval of 20 min. The concentration of aqueous methyl orange was determined by scanning the absorbance of the sample within the scope of 200-600 nm with a UV-VIS spectrophotometer.

3 Results and analysis

3.1 Photooxidation activity

The activity of the photocatalyst was analyzed on the basis of photocatalytic reactions of aqueous methyl orange. In 80 min, the degradation rate of aqueous methyl orange was 62%, 12% and 34% for Mn non-uniformly doped film (0.7%), the uniformly doped film (0.7%) and pure titanium dioxide film, respectively. The kinetics equation can be expressed as [13,14]

$$\ln(c_0/c) = K_{\text{obs}} t_{\text{illum}}$$

where K_{obs} is the apparent rate constant, t_{illum} is the reaction time, and c_0 and c are the concentration of methyl-orange at initial time and the time t_{illum} , respectively.

Fig.1 shows the comparison of activities of TiO_2 films doped non-uniformly(MT) and uniformly(MM) by Mn at the doping concentration of 0.7%, with that of pure TiO_2 films(TT). Although the photocatalytic activity of MM films is evidently worse than that of TT, the activity of MT films is higher than that of TT. We further determined the optimal dopant concentration in MT mode to be about 0.7% (Fig.2).

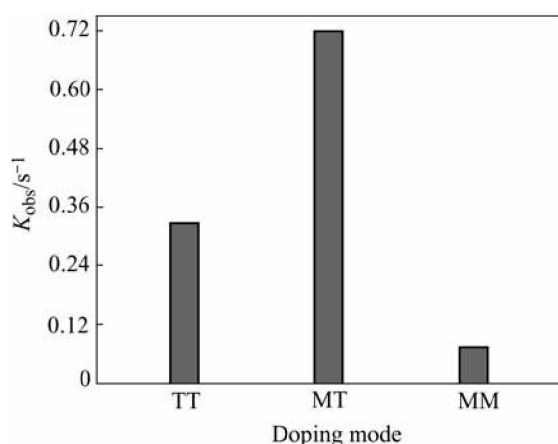


Fig.1 Apparent parameter of methyl orange degradation kinetics vs doping mode

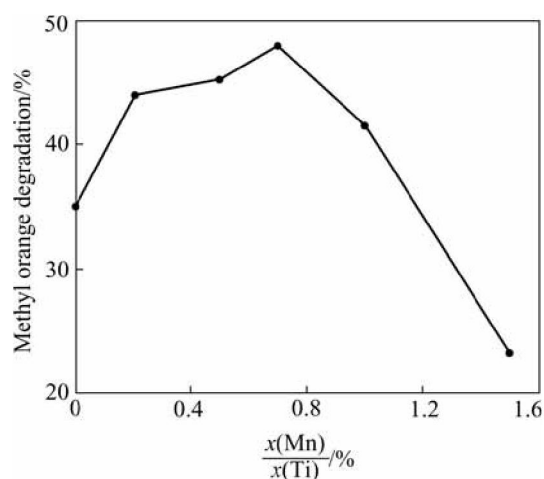


Fig.2 Variation of degradation rate with Mn dopant concentration in MT mode

3.2 UV-vis absorbency spectra

For the doped TiO_2 , when Ti^{4+} is substituted by Mn^{4+} within the crystal lattice of TiO_2 , an impurity level will be formed in the forbidden region near the bottom of the conduction bands. The band gap will be therefore narrowed, which results in an increase of photon-

generated carriers inside the doped TiO_2 . The UV-vis absorbency spectra of the Mn-doped films and the pure TiO_2 films are compared in Fig.3. The absorption edges of TiO_2 doped by Mn in both MT and MM modes reveal a "red shift".

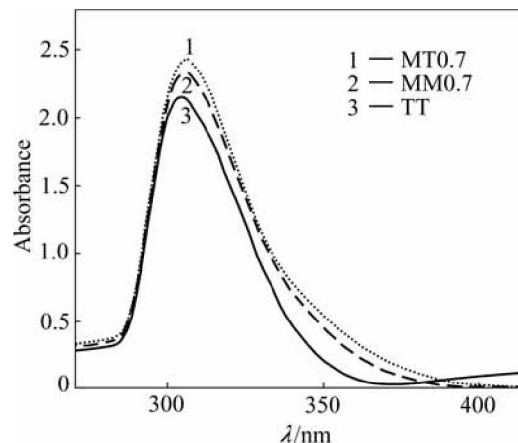


Fig.3 UV-vis absorbency of Mn doped and pure TiO_2 films

3.3 Analysis by SEM and XPS

The thickness of the films was measured by scanning electron microscopy(SEM) after the cross-sections were sprayed with carbon film in a vacuum plating instrument. A typical SEM micrograph of cross-section of the TiO_2 film is shown in Fig.4. The thickness of the film is about 350 nm.



Fig.4 SEM image of film cross-section

The information around an atom, such as the change of charge density and chemical valence, can be examined by the chemical shift detected by X-ray photoelectron spectroscopy changes. Because the amount of incorporated manganese is too little, its signal can not be directly detected by this equipment. Therefore we measured the change of the binding energy of O1s in different depths of the film to observe the effect of the Mn doping. Then we compared the change of binding energy of O1s in different depths of the film (doped by Mn with nonuniform distribution at 0.7%) via the erosion of Ar^+ and XPS. The fitting curve of O1s in different depths of the film is shown in Fig.5. The BE (binding

energy) of 530.0 eV is considered to be the oxygen at crystal lattice, the BE beyond 532.0 eV is the adsorbing oxygen, and the BE between 530.0 eV and 532.0 eV is hydroxyl oxygen[15]. The fitting curve of O1s on the surface of the film was created according to Ref.[15]. At the 100 nm depth of the film, there are only two fitting peaks of O1s, 530.6 eV and 529.6 eV, respectively, one of which may be from the oxygen in the O—Mn and the other one from that in the O—Ti.

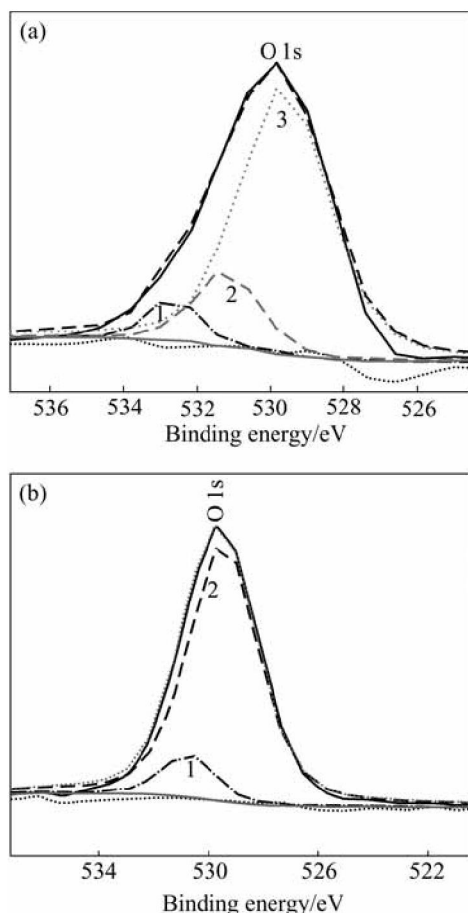


Fig.5 XPS spectra of O1s in different depths of film: (a) Fitted O1s spectrum of TiO_2 on surface (Peak 1 is adsorbed O_2 or H_2O ; Peak 2 is O—H; Peak 3 is O—Ti); (b) Fitted O1s spectrum of $\text{MnO}_2/\text{TiO}_2$ in 100 nm (Peak 1 is O—Mn; Peak 2 is O—Ti)

3.4 Verification of PN junction in film doped non-uniformly by Mn

The electrochemical properties of photocatalyst films were analyzed in a three electrode system with a light on/off shutter using a CHI660 electrochemical station.

3.4.1 Response characteristic of ITO glass with UV irradiation under different bias voltage values

The response characteristic of ITO glass under various forward bias and reverse bias is shown in Fig.6. Taking the noise signal of the instrument into consideration, it is found that there is basically no

response signal of photocurrent in the ITO glass with UV irradiation.

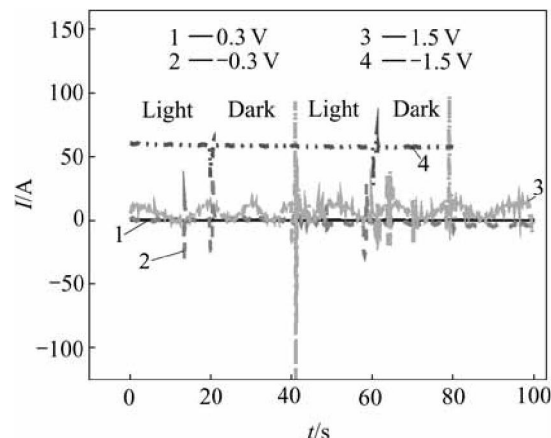


Fig.6 Amperometric current of ITO glass electrodes vs time

3.4.2 Photocurrent of Mn non-uniformly doped TiO_2 film under various bias voltages values

The PN junction exhibits the characteristic of capacitance-tension, which is affected by potential barrier capacitance and diffusion capacitance. The potential barrier capacitance is formed by ion lamina in the space-charge region of semiconductor, and the diffusion capacitance is formed by the major carriers of the semiconductor. When the additional bias voltage is changed, the width of the space-charge region and the diffusion current (i.e. current circuit) of semiconductor are changed accordingly, similar to the situation when the capacitance charges and discharges[16].

Fig.7 shows the response signal of photocurrent of the film (MT) at 0.7% with the light on/off shutter under different bias voltage values. With the forward bias enhanced within 1.0 V, the intensity of photocurrent increases gradually. After the forward bias reaches 1.0 V, the signal of photocurrent barely increases following the increasing forward bias. However, with the reverse bias

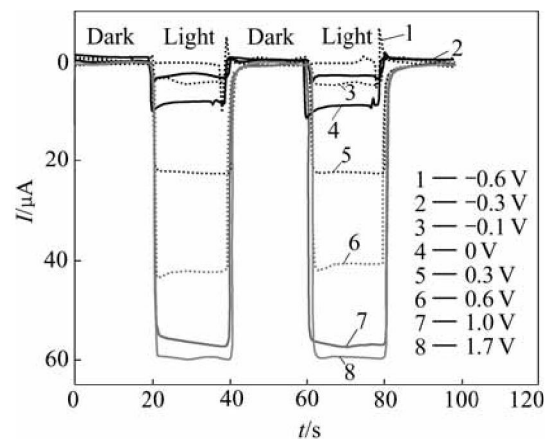


Fig.7 Amperometric current vs time of Mn-doped (MT mode) TiO_2 film electrodes at 0.7% under various bias voltage values

enhanced, the intensity of the photocurrent decreases gradually. The noise signal of the instrument also appears. When the reverse bias increases to -0.6 V, the signal of photocurrent nearly disappears. This indicates that the Mn non-uniformly doped titanium dioxide film exhibits the property of a PN junction.

3.4.3 Photocurrent of Mn-doped uniformly TiO_2 film under various bias voltage values

To verify the structure of MM films, we carried out the following test. Fig.8 shows the response signal of photocurrent of the film (MM) at 0.7% with the light on/off shutter under the bias voltage of ± 0.3 V. When the circuit is applied to the same intensity of forward bias and reverse bias, the intensity of photocurrent is the same if one excludes the noise signal of the instrument; compared with Fig.7, it is obvious that a PN junction does not form in the MM film.

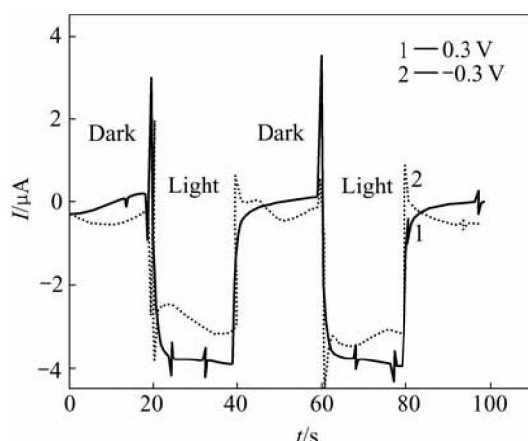


Fig.8 Amperometric current vs time of Mn-doped (MM mode) TiO_2 film electrodes at 0.7% under bias voltage values of 0.3 V and -0.3 V.

3.5 Analysis of separation of photon-generated carriers

The transient photon-currents were analyzed using a CHI660 electrochemical station. Under the UV radiation, when the transient photon-current is measured, a cathode photocurrent signal is generated because of the transition of photoelectrons from valence band to conduction band [17]. This reflects the conductance value and the number of free current carriers in the semiconductor, and the photon-generated carriers diffuse onto the electrode/solution interface. Fig.9 shows the chart of transient photocurrent in doped and pure TiO_2 electrode systems. The signals of transient photocurrent of MT electrode system are stronger than those of pure TiO_2 electrode (TT), whereas the signals of MM electrode are weaker than those of pure TiO_2 . This indicates that the number of free current carriers in the MT film is much more than those in the TT or MM film under the UV radiation.

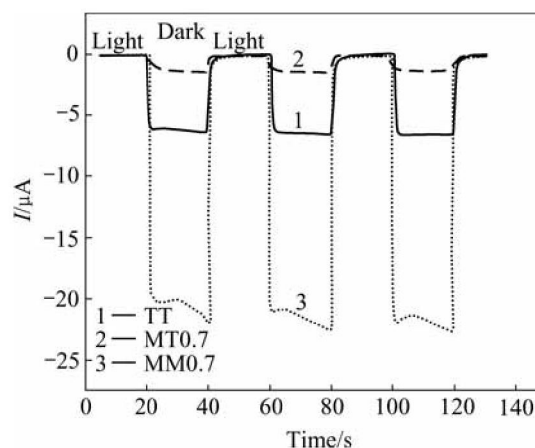


Fig.9 Amperometric current curve vs time for doped (0.7%) and pure TiO_2 film electrodes

3.6 Effect of ethanol in electrolyte on transient photoelectric current of film electrode

Under the UV radiation, a great deal of current carriers are excited in the film, and the carriers can be separated effectively. To investigate the migration of the photon-generated carriers on the surface of the film, we added ethanol into the electrolyte. Without bias voltage or the same forward bias, the photon-generated carrier can migrate and the signal of the photocurrent is intensified greatly after ethanol is added into the electrolyte (Fig.10).

Fig.11 presents the photocurrent curves of Mn-doped (MT mode) TiO_2 film electrodes at 0.7% under various forward bias values in ethanol-addition electrolytes. As the forward bias increases, the signal of photocurrent intensifies sharply at the beginning; but after the forward bias reaches 0.3 V, it stays at the platform even when the forward bias continues to increase. Compared with Fig.7, when the ethanol is not included in the electrolyte, this forward bias is 1.0 V. Many factors affect the electrode current. For this experiment system, the main factors are the surface reaction and the migration of the current carrier on the surface [18]. If the electrons are the major carriers, their migration will experience a series of reactions, including protonation; if the holes are the major carriers, they may oxidize the organic matter adsorbed to the surface of the electrode and migrate simultaneously. Because the flux of the matter on the electrode surface controls the reaction speed and the external current [18], the signal of photocurrent is intensified rapidly. Therefore we can conclude that the major carriers on the TiO_2 films are holes.

4 Discussion

Titania is an n-type semiconductor because of the presence of oxygen atom vacancies [19,20]. For the Mn-

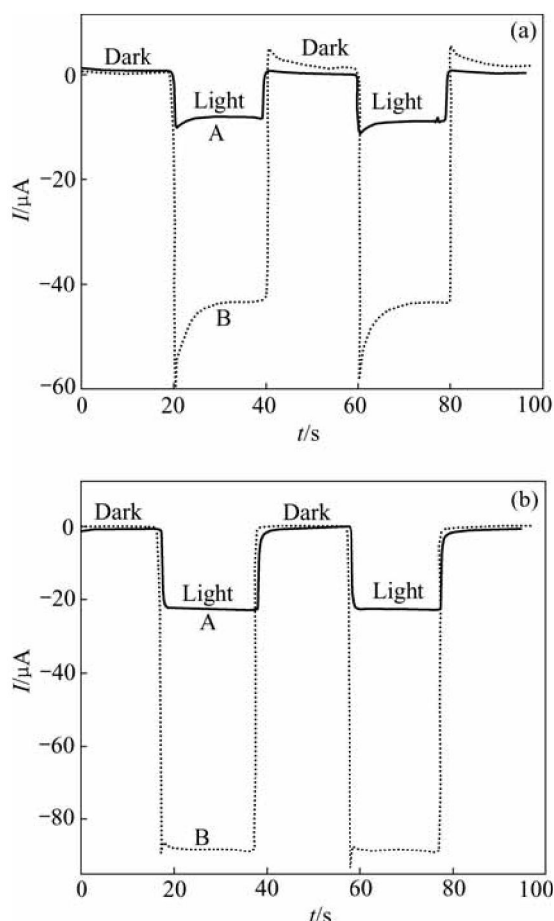


Fig.10 Amperometric current vs time of Mn-doped TiO_2 film (MT) electrodes at 0.7% in different electrolyte under different bias voltage values: (a) Bias voltage 0 V; (b) Bias voltage 0.3 V; A 0.01 mol/L Na_2SO_4 ; B 0.01 mol/L $\text{Na}_2\text{SO}_4 + \text{CH}_3\text{CH}_2\text{OH}$

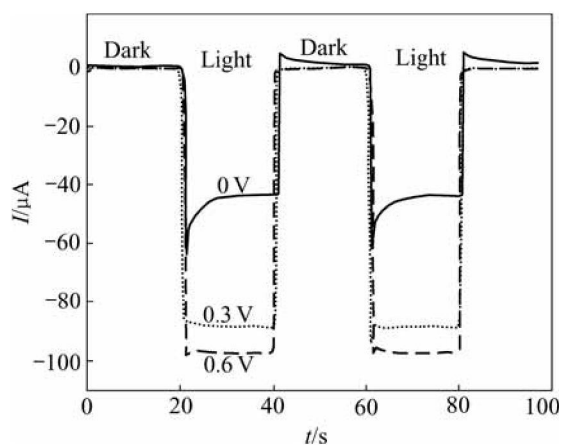


Fig.11 Amperometric current vs time of Mn-doped (MT mode) TiO_2 film electrodes at 0.7% under various forward bias values in ethanol-addition electrolytes

doped films by the MT mode, when the films are heat-treated, the solid solution of Mn/TiO_2 is formed in the films and a concentration gradient from bottom layer

to surface layer in the film is generated, due to the diffusion and migration of Mn ions (Fig.12). Mn ion exists as Mn^{4+} after Mn-doped TiO_2 is treated at 500 °C [21]. The configuration of the extra-nuclear electron of Mn^{4+} is $3s^23p^63d^3$, which tends to return to $3s^23p^63d^5$ (Mn^{2+}), which is stably associated with the half-filled subshells ($3d^5$). With UV radiation, there are photon-generated carriers within the semiconductor. The Mn^{4+} in the bottom layer becomes the electron acceptor, and the photon-generated electrons transfer from surface layer to bottom layer in the films. Thus the PN junction is formed in the doped TiO_2 film with N-type fields in the bottom layer and P-type fields in the surface layer. When the diffusion of the carriers reaches equilibrium, each Fermi level in the system is at the same level, but the band near the interface bends and forms a potential barrier of current carriers, namely, a space-charge region[22,23]. The potential barrier suppresses the recombination of the electron-hole pairs, which is indicated by the photocurrent signal (Fig.9). In the photocatalytic oxidation reaction, when the holes on the surface are consumed, the holes near the interface in the bottom layer will migrate to the surface layer because of the effect of the electric field of potential barrier, so the concentration of holes in the surface layer increases and the photocatalytic activity is enhanced.

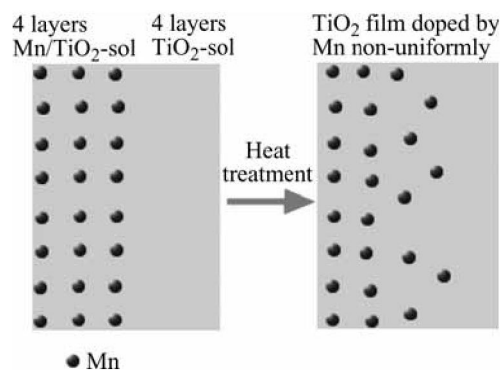


Fig.12 Diagrammatic sketch of Mn non-uniform distribution in MT film

For Mn/TiO_2 films doped in MM mode, the sites of dopant ions may become electron-hole recombination centers, which will greatly decrease the lifetime of the charge carriers. More importantly, it can not form a potential barrier; therefore, the photocatalytic activity decreases accordingly.

5 Conclusions

Based on the peculiarity and technology of semiconductor devices, the catalysts films of TiO_2 with high photocatalytic activity, doped by Mn with non-uniform distribution, are designed and prepared by a

sol-gel method under process control. The results of the electrochemical test prove that the PN junction is formed in the Mn-doped uniformly titanium dioxide film; and the photocatalytic activity of the TiO_2 prepared by this novel method is enhanced greatly. A mechanism is discussed in term of the effective separation of current carrier, which is demonstrated by transient photoelectric current and open circuit potential.

Acknowledgment

The authors would like to thank Dr. Feng LIU from University of California at Irvine and Dr. Kohichi SEGAWA from Sophia University for their help in correcting our English writing.

References

- [1] MARTRA G. Lewis acid and base sites at the surface of microcrystalline TiO_2 anatase: relationships between surface morphology and chemical behaviour [J]. *Applied Catalysis A—General*, 2000, 200(1/2): 275–285.
- [2] YE F X, OHMORI A. A new application field of plasma spraying technique to environmental depollution [J]. *Trans Nonferrous Met Soc China*, 2004, 14(S1): 55–61.
- [3] PENG B, YUAN C, CHAI L Y, WEI S W, YU Y F, SU W F. Preparation of titanium dioxide/silver sulfate powder and its antibacterial activity [J]. *Trans Nonferrous Met Soc China*, 2005, 15(5): 1156–1160.
- [4] XIN B F, REN Z Y, HU H Y, ZHANG X Y, DONG C L, SHI K Y, JING L Q, FU H G. Photocatalytic activity and interfacial carrier transfer of Ag- TiO_2 nanoparticle films [J]. *Applied Surface Science*, 2005, 252(5): 2050–2055.
- [5] GUAN K S, XU H, LU B J. Hydrophilic property of SiO_2 - TiO_2 overlayer films and $\text{TiO}_2/\text{SiO}_2$ mixing films [J]. *Trans Nonferrous Met Soc China*, 2004, 14(2): 251–254.
- [6] SOPYAN I, MURASAWA S, HASHIMOTO K, FUJISHIMA A. Highly efficient TiO_2 film photocatalyst-degradation of gaseous acetaldehyde [J]. *Chemistry Letters*, 1994(4): 723–726.
- [7] ILEPERUMA O A, TENNAKONE K, DISSANAYAKE W D D P. Photocatalytic behavior of metal doped titanium-dioxide—Studies on the photochemical-synthesis of ammonia on Mg/ TiO_2 catalyst systems [J]. *Applied Catalysis*, 1990, 62(1): L1–L5.
- [8] CHOI W Y, TERMIN A, HOFFMANN M R. The role of metal-ion dopants in quantum-sized TiO_2 -correlation between photoreactivity and charge-carrier recombination dynamics [J]. *Journal of Physical Chemistry*, 1994, 98(51): 13669–13679.
- [9] BREZOVA V, BLAZKOVA A, KARPINSKY L. Phenol decomposition using $\text{M}^{n+}/\text{TiO}_2$ photocatalysts supported by the sol-gel technique on glass fibres [J]. *Journal of Photochemistry and Photobiology A—Chemistry*, 1997, 109(2): 177–183.
- [10] DI PAOLA A, GARCIA-LOPEZ E, IKEDA S, MARCI G, OHTANI B, PALMISANO L. Photocatalytic degradation of organic compounds in aqueous systems by transition metal doped polycrystalline TiO_2 [J]. *Catalysis Today*, 2002, 75(1–4): 87–93.
- [11] ASSABANE A, ICHOU YA, TAHIRI H, GUILLARD C, HERRMANN J M. Photocatalytic degradation of polycarboxylic benzoic acids in UV-irradiated aqueous suspensions of titania. Identification of intermediates and reaction pathway of the photomineralization of trimellitic acid (1,2,4-benzene tricarboxylic acid) [J]. *Applied Catalysis B—Environmental*, 2000, 24(2): 71–87.
- [12] YANG Y, LI X J, CHEN J T, WANG L Y. Effect of doping mode on the photocatalytic activities of Mo/ TiO_2 [J]. *Journal of Photochemistry And Photobiology A—Chemistry*, 2004, 163(3): 517–522.
- [13] ZHANG Y, CRITTENDEN J C, HAND D W, PERRAM D L. Fixed-bed photocatalysts for solar decontamination of water [J]. *Environmental Science and Technology*, 1994, 28(3): 435–442.
- [14] MATTHEWS R W. Kinetics of Photocatalytic oxidation of organic Solutes over titanium dioxide [J]. *Journal of Catalysis*, 1988, 111: 264–272.
- [15] YANG X G, SHENG S S. The XPS study on the composite $\text{LaMn}_{1-x}\text{Fe}_x\text{O}_3$ ($x=0-1$) [J]. *Acta Phys Chem Sin*, 1995, 11(8): 681–687.
- [16] GROVE A S. *Physics and Technology of Semiconductor Devices* [M]. New York: John Wiley & Sons, Inc, 1976: 158.
- [17] YE F X, OHMORI A, LI C J. New approach to enhance the photocatalytic activity of plasma sprayed TiO_2 coatings using p-n [J]. *Surface and Coatings Technology*, 2004, 184(2/3): 233–238.
- [18] BARD A J, FAULKNER L R. *Electrochemical Methods, Fundamentals and Applications* [M]. New York: John Wiley & Sons, Inc, 1980.
- [19] KINGERY W D, BOWEN H K, UHLMANN D R. *Introduction to Ceramics* [M]. 2nd ed. New York: John Wiley & Sons, 1976.
- [20] ZENG R J. *The Chemistry of Inorganic Materials* [M]. Xiamen: Xiamen Univ Press, 2001.
- [21] DING S W, WANG L Y, ZHANG S Y, ZHOU Q X, DING Y, LIU S J, LIU Y C, KANG Q Y. Hydrothermal synthesis, structure and photocatalytic property of nano- TiO_2 - MnO_2 [J]. *Science in China Series B—Chemistry*, 2003, 46(6): 542–548.
- [22] WANG Y Q, CHENG H M, MA J M. The photoelectrochemical properties of composite titanium dioxide and ferric oxide nanocrystalline electrodes [J]. *Acta Physico-Chimica Sinica*, 1999, 15(3): 222–227.
- [23] XU W, LI X J, ZHENG S J, WANG J G. Comparison of photocatalytic activity of TiO_2 film doped nonuniformly by Mn and Zn [J]. *Trans Nonferrous Met Soc China*, 2005, 15(5): 1194–1198.

(Edited by YUAN Sai-qian)